

## 8-Phenyl-Substituted Dipyrromethene·BF<sub>2</sub> Complexes as Highly Efficient and Photostable Laser Dyes

I. García-Moreno,\* A. Costela, and L. Campo

*Instituto de Química-Física “Rocasolano”, C.S.I.C., Serrano 119, 28006 Madrid, Spain*

R. Sastre

*Instituto de Ciencia y Tecnología de Polímeros, C.S.I.C., Juan de la Cierva 3, 28006 Madrid, Spain*

F. Amat-Guerri and M. Liras

*Instituto de Química Orgánica, C.S.I.C., Juan de la Cierva 3, 28006 Madrid, Spain*

F. López Arbeloa, J. Bañuelos Prieto, and I. López Arbeloa

*Departamento de Química-Física, UPV-EHU, Apartado 644, 48080 Bilbao, Spain*

*Received: November 13, 2003*

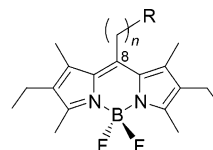
We report on the synthesis and the photophysical and lasing properties of two new dipyrromethene·BF<sub>2</sub> dyes, analogues of the commercial dye PM567, dissolved in liquid solutions or in polymeric matrices of poly(methyl methacrylate) and as solid copolymers with methyl methacrylate, where the chromophore is covalently bound to the polymeric chains. The new dyes have the 8 position substituted by the group *p*-(acetoxypolymethylene)phenyl or *p*-(methacryloyloxypolymethylene)phenyl (number of methylenes = 1 or 3). Good correlations between the photophysical properties in dilute solutions and the lasing characteristics in moderately concentrated solutions have been observed. The presence of the 8-phenyl substituent does not significantly modify the photophysics of the chromophore. Theoretical calculations were performed to rationalize this behavior. Under transversal pumping at 534 nm, laser efficiencies up to 46% were obtained for liquid solutions, which were found to be nearly independent of the nature of the solvent and the length of the polymethylene chain. For solid samples, lasing efficiencies of up to 23% and good photostabilities, with 96% of the initial laser output after 100 000 pump pulses at 10 Hz, were established.

### I. Introduction

As a result of the continuous effort to produce improved dyes for laser applications, in the late 1980s Pavlopoulos, Boyer, and co-workers developed the dipyrromethene·BF<sub>2</sub> (P·BF<sub>2</sub>) dyes. This new family of dyes promised enhanced lasing efficiency and photostability<sup>1–6</sup> because they exhibited high fluorescence quantum yields owing to their low triplet (T–T) absorption losses at the fluorescence emission wavelengths.<sup>7,8</sup> However, when reviewing the spectroscopic and photochemical parameters of the P·BF<sub>2</sub> complexes, one concludes that these dyes are not yet the ultimate high-efficiency and photostable laser dyes because they are not stable enough for the required uses and are particularly sensitive to photoreactions with oxygen.<sup>9</sup> In trying to improve the lasing performance of these dyes, recent studies have demonstrated that adequate substituents in the molecular core can enhance the laser action.<sup>10</sup>

Special attention has been paid to the dye 1,3,5,7,8-pentamethyl-2,6-diethyl dipyrromethene·BF<sub>2</sub> (PM567, Scheme 1) because of the simplicity of its chemical structure and its good laser performance in both the liquid and solid state.<sup>11,12</sup> The photophysical behavior and the photochemical stability of this dye can be modulated by changes in the substitution pattern on the tricyclic ring system. Over the last few years, we have

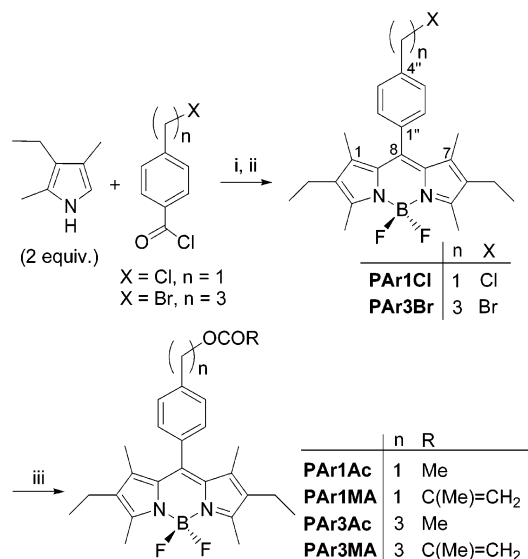
### SCHEME 1: Molecular Structures of the PM567 Dye and the PnAc and PnMA Analogues



	R	n
PM567	H	1
PnAc	OCOMe	1,3,5,10,15
PnMA	OCOC(Me)=CH <sub>2</sub>	1,3,5,10,15

studied the effect of introducing a number of substitutions at the 8 position of this molecule while maintaining the four methyl groups in the 1, 3, 5, and 7 positions and the ethyl groups in positions 2 and 6.<sup>13–16</sup> The presence of an 8-(*ω*-acetoxypolymethylene or an 8-(*ω*-methacryloyloxy)polymethylene substituent (dyes PnAc and PnMA, respectively; Scheme 1) does not significantly modify the photophysics of the chromophore with regard to that of PM567, especially if the linear polymethylene chain has five or more methylene groups.<sup>14</sup> These new dyes, when dissolved in a variety of organic solvents, lased more efficiently than PM567 and, under continuous UV irradiation, demonstrated improved photostability.<sup>13,15</sup> In addition, these newly synthesized analogues of PM567, either dissolved in poly(methyl methacrylate) (PMMA) or covalently bound to methyl

\* Corresponding author. E-mail: iqrfm84@iqfr.csic.es.

**SCHEME 2: Synthesis of the New Dipyrromethene·BF<sub>2</sub> Dyes PArnAc and PArnMA<sup>a</sup>**


<sup>a</sup> Conditions: (i) CH<sub>2</sub>Cl<sub>2</sub>, Ar, 50 °C, 2 h; (ii) Et<sub>3</sub>N, MePh-CH<sub>2</sub>Cl<sub>2</sub>, 95:5, Ar, room temperature, 30 min, followed by BF<sub>3</sub>·Et<sub>2</sub>O, 50 °C, 1.5 h; (iii) MeCO<sub>2</sub>Na (for PArnAc dyes) or CH<sub>2</sub>=C(Me)CO<sub>2</sub>K (for PArnMA dyes), DMF, Ar, 1–20 h.

methacrylate (MMA), lased more efficiently than the parent dye PM567 incorporated into PMMA. Once more, the photophysical properties of PM567 were not significantly modified by the substituents, except that the fluorescence quantum yield of some solid samples increased to up to 0.89.<sup>16</sup>

In light of the former results, the question that arises is whether the presence of other 8-substituent groups in the PM567 chromophore core, such as a phenyl group, could enhance its photophysical properties and lasing performance in both liquid and solid phases. Initially, we speculated that an 8-phenyl-substituted molecular structure might be less sensitive to chemical reactions with oxygen. This fact, together with the ability of this structure to modify the degree of polarization under excitation, which facilitates the dissipation of the absorbed energy not converted into emission, should render more photostable dyes that are valuable for solid-state lasers.

The photophysical properties of some 8-phenyl P·BF<sub>2</sub> dyes previously described in the literature are controversial. Pavlopoulos et al. synthesized the 1,3,5,7-tetramethyl-8-(*p*-methoxy)phenyl-P·BF<sub>2</sub> dye and concluded that this substitution does not result in any significant improvement of the laser action properties because it brings a blue shift as well as an intensification of the T–T absorption over the fluorescence spectral region.<sup>7</sup> Recently, Liang et al. reported the spectroscopic and laser action properties of three 1,3,5,7-tetramethyl-2,6-diethyl-P·BF<sub>2</sub> dyes with phenyl, *p*-methoxyphenyl, and *p*-fluorophenyl substituents at the 8 position.<sup>17</sup> They concluded that their corresponding T–T absorption values are rather low over their fluorescence spectral regions and that they, along with their high fluorescence quantum yields, are the main factors that enable these laser dyes to perform efficiently.

To develop improved laser dyes and in an attempt to clarify this controversy, we have synthesized new P·BF<sub>2</sub> dyes with the same substituents as PM567 in positions 1 to 7 but containing at position 8 a *p*-(acetoxypolymethylene)phenyl group with 1 or 3 methylene groups (dyes PArnAc, Scheme 2) or a *p*-(methacryloyloxypolymethylene)phenyl group with the same number of methylenes (dyes PArnMA). The PArnAc dyes are model compounds of the PArnMA monomers. In this paper,

we have proceeded to characterize properly the photophysical and lasing properties of these new dyes in air-equilibrated liquid solutions of apolar, polar nonprotic, and polar protic solvents, paying attention to the effect of the dye concentration. To gain deeper insight into the characteristics of these high-emitting dyes, we have also studied their properties in the solid state either by the copolymerization of PArnMA monomers with MMA, yielding solid copolymers COP(PArnMA-MMA) where the covalently bound chromophore is separated from the polymeric chain by a polymethylenephenyl group, or simply by dissolving the PArnAc model dyes into PMMA, rendering materials named PArnAc/PMMA.

## II. Experiment

**Materials.** PM567 (laser grade, from Exciton) was used as received. The purity of the dye was found to be >99%, as determined by spectroscopic and chromatographic methods. All solvents (Merck, Aldrich, or Sigma) were spectroscopic grade and were used without further purification. Methyl methacrylate (MMA, Aldrich, 99% purity) was successively washed with 5% NaOH in water and pure water and then dried over Na<sub>2</sub>SO<sub>4</sub> and distilled under reduced pressure. 2,2'-Azobis(isobutyronitrile) (AIBN, from Merck) was crystallized in the dark from methanol. Chemicals were purchased from Aldrich and were used without further purification. *p*-(3-Bromopropyl)benzoyl chloride was obtained in three steps from (1) the 1-bromo-3-phenylpropane (25 mmol) reaction with acetyl chloride to yield *p*-(3-bromopropyl)acetophenone (yield 90%);<sup>18</sup> (2) the conversion of this acetophenone into *p*-(3-bromopropyl)benzoic acid with Br<sub>2</sub>/NaOH (yield 64%);<sup>19,20</sup> and (3) the treatment of the resulting carboxylic acid with thionyl chloride.

**Synthesis of Precursors PAr1Cl and PAr3Br.** *p*-(Chloromethyl)benzoyl chloride (1.5 g, 8 mmol) or *p*-(3-bromopropyl)benzoyl chloride (2.1 g, 8 mmol), respectively, was added dropwise to a stirred solution of freshly distilled 2,4-dimethyl-3-ethylpyrrole (2.2 mL) in dichloromethane (90 mL) at room temperature and under Ar, and the mixture was heated to 50 °C with stirring for 2 h. After the vacuum evaporation of the solvent, toluene (190 mL), dichloromethane (10 mL), and triethylamine (3.88 g, 38 mmol) were added to the residual solid, the mixture was stirred at room temperature for 30 min under Ar, and boron trifluoride diethyl etherate (7.82 g, 55 mmol) was then added. After heating to 50 °C for 1.5 h, the subsequent workup yielded a residue that was purified by column chromatography (silica gel, hexanes–EtOAc mixtures as eluents) and crystallization from hexane at –78 °C. For data, see the Appendix.

**Synthesis of Models PArnAc and Monomers PArnMA.** A solution of sodium acetate (1 mmol) or potassium methacrylate (1 mmol) and PAr1Cl (0.25 mmol) or PAr3Br (0.25 mmol) in DMF (30 mL) was stirred at room temperature for 5–7 days or at 40 °C for 1–20 h under an Ar atmosphere and in the dark. The subsequent workup yielded a residue that was purified by column chromatography (silica gel, hexanes–EtOAc 98:2 to 80:20) and crystallization from hexane at –78 °C. For data, see the Appendix.

**Preparation of Solid Polymeric Samples.** The dyes were incorporated into solid matrices of methyl methacrylate (MMA) following the procedure previously described.<sup>15</sup>

**Laser Experiments.** Liquid solutions of dyes were contained in 1-cm optical-path quartz cells that were carefully sealed to avoid solvent evaporation during the experiments. The solid samples for laser experiments were cast in a cylindrical shape, forming rods of 10-mm diameter and 10-mm length. A cut was

made parallel to the axis of the cylinder to obtain a lateral flat surface of ca.  $4 \times 10 \text{ mm}^2$ . This surface was prepared for lasing experiments by conventional grinding and polishing. The ends of the laser rods were also hand-polished to an optical-grade finish. The samples were transversely pumped at 534 nm with 5.5-mJ, 6-ns fwhm pulses from a frequency-doubled Q-switched Nd:KGW laser (Monocrom STR-2+) at a repetition rate of up to 10 Hz. Details of the experimental system can be found elsewhere.<sup>21</sup>

**Photophysical Properties.** Photophysical properties of dilute solutions ( $2 \times 10^{-6} \text{ M}$ ) were measured in 1-cm optical path length quartz cuvettes. Fluorescence quantum yields ( $\phi$ ) were determined using a dilute solution of PM567 in methanol as a reference ( $\phi = 0.91$ ).<sup>22</sup> The fluorescence decay curves were analyzed as monoexponentials ( $\chi^2 < 1.3$ ), and the fluorescence decay time ( $\tau$ ) was obtained from the slope.

For concentrated solutions (up to  $10^{-3} \text{ M}$ ), 0.01- and 0.001-cm path length cuvettes were employed, and to reduce the reabsorption and reemission effects,<sup>23</sup> the emission signals were recorded in the front-face configuration, orientating the cuvette 35 and 55° with respect to the excitation and emission beams, respectively. Samples in 0.001-cm cuvettes were carefully manipulated to avoid solvent evaporation and to get reproducible fluorescence intensities. Indeed, the reported fluorescence quantum yields are always the average of at least three independent measurements.

Photophysical properties of solid polymeric samples were measured from disk-shaped samples with a thickness of 0.2 mm and a dye concentration of  $1.5 \times 10^{-3} \text{ M}$ . Absorption was registered in transmittance, and fluorescence measurements were recorded by employing the above-mentioned front-face setup. Fluorescence quantum yields were determined by using a solid disk of the dye PM567 in a copolymer of trifluoromethyl methacrylate (30%) and methyl methacrylate (70%)<sup>24</sup> as a reference. All measurements were performed at  $20 \pm 0.2 \text{ }^\circ\text{C}$ .

**Theoretical Calculations.** These were performed with the MOPAC 2000 (Fujitsu) method. The semiempirical AM1 method was recommended for the geometry optimization of the dyes instead of the more commonly used semiempirical PM3 method because of the unsatisfactory parametrization of the boron atom in the latter method.

### III. Results and Discussion

**Photophysical Properties in the Liquid Phase.** The photophysical characteristics of the new dyes in liquid solution were studied in polar protic (2,2,2-trifluoroethanol, ethanol, and methanol), polar nonprotic (acetone and ethyl acetate), and apolar (cyclohexane) solvents. The absorption and fluorescence spectra of dyes PAR1Ac and PAR3Ac in ethanol solution are shown in Figure 1, where the absorption spectrum of PM567 in the same solvent is also included for comparison. Both the absorption and the fluorescence bands of the 8-phenyl-substituted analogues are bathochromically shifted (around 5 nm) with respect to those of PM567.<sup>25</sup> The shape and position of the absorption and fluorescence bands are similar in both 8-phenyl dyes and are reminiscent of the corresponding bands observed in PM567. The absorption and fluorescence intensities are slightly lower than those of PM567, mainly in the fluorescence emission. The fluorescence decay curves of PAR1Ac and PAR3Ac in dilute solution are analyzed as one-exponential decays (Figure 2) with a lifetime of around 5–6 ns, which is close to that of PM567 in dilute solution.

These results suggest that the presence of the 8-phenyl substituent does not extensively affect the photophysical proper-

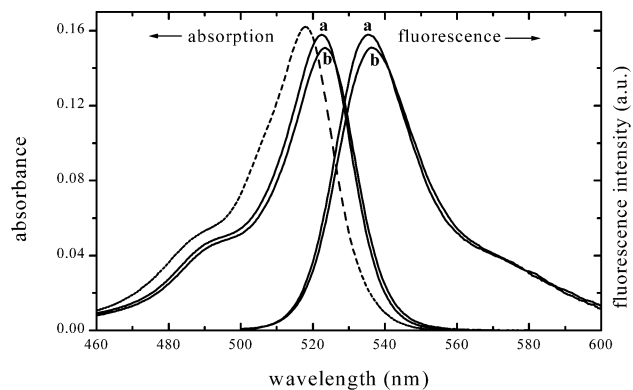


**Figure 1.** Absorption and corrected fluorescence spectra of dilute solutions ( $2 \times 10^{-6} \text{ M}$ ) of (a) PAR3Ac and (b) PAR1Ac dyes in ethanol. The absorption spectrum of PM567 in ethanol (---) is also included for comparison.

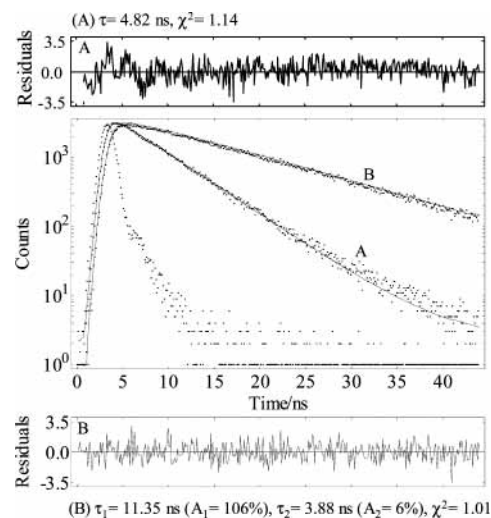


**Figure 2.** Fluorescence decay curves of (A) PAR1Ac in dilute solution in acetone, analyzed as a one exponential ( $\tau = 4.82 \text{ ns}$  with  $\chi^2 = 1.14$ ), and (B) COP(PAR1MA-MMA) analyzed as growing ( $\tau_1 = 3.88 \text{ ns}$ ) and decaying ( $\tau_2 = 11.35 \text{ ns}$ ) ( $\chi^2 = 1.01$ ).

ties of P·BF<sub>2</sub> dyes and rule out any possible intramolecular interaction between the  $\pi$  electrons of the phenyl group and the P·BF<sub>2</sub> chromophoric core affecting their photophysics.<sup>26</sup> Theoretical calculations corroborate this assumption. Figure 3 shows the geometry of the ground state of the PAR3Ac dye optimized by the AM1 semiempirical method in which the phenyl ring is in a nearly perpendicular conformation with respect to the boron–dipyrromethene plane. Experimental data obtained by single-crystal X-ray diffraction confirm this geometry.<sup>27</sup> Such conformation is a consequence of the geometrical restrictions imposed by the two methyl groups in the 1 and 7 positions<sup>28–31</sup> because an 8-aromatic substituent in the P·BF<sub>2</sub> chromophore without 1- and 7-methyl groups leads to important changes in the fluorescence properties owing to the nearly planar conformation of both  $\pi$  systems in the excited state.<sup>30</sup>

The photophysical properties of dilute solutions of PAR1Ac are similar to those of PAR3Ac in a common solvent (Table 1), with only a slight bathochromic shift (around 1 nm) in both the absorption and fluorescence bands of PAR3Ac with respect to PAR1Ac and a slight increase in the molar absorption coefficient and fluorescence quantum yield and lifetime (which is reflected in a slight increase in the fluorescence processes probability,  $k_f$ ) in the former dye. These results indicate that the length of the linking polymethylene chain at the para position of the phenyl group does not affect the photophysics of the chro-

**TABLE 1: Photophysical and Lasing Properties of the PArAc Dyes in Several Solvents<sup>a</sup>**

solvent	$\lambda_{ab}$ ( $\pm 0.1$ nm)	$\epsilon_{max} \times 10^{-4}$ ( $M^{-1} cm^{-1}$ )	$\lambda_{fl}$ ( $\pm 0.4$ nm)	$\phi$ ( $\pm 0.05$ )	$\tau$ ( $\pm 0.05$ ns)	$k_{fl}$ ( $10^8 s^{-1}$ )	$k_{nr}$ ( $10^8 s^{-1}$ )	$\lambda_{la}$ (nm)	%eff
PAr1Ac									
F <sub>3</sub> -ethanol <sup>b</sup>	521.6	6.56	535.2	0.81	6.35	1.27	0.30	552	43
methanol	522.3	7.38	535.6	0.71	5.18	1.37	0.56	556	41
ethanol	523.6	7.53	536.0	0.68	5.18	1.31	0.62	555	43
acetone	522.2	7.02	536.0	0.65	4.82	1.34	0.73	554	44
ethyl acetate	522.6	7.59	536.0	0.65	5.00	1.30	0.70	554	42
c-hexane	526.0	8.05	538.0	0.45	3.68	1.22	1.49	555	40
PAr3Ac									
F <sub>3</sub> -ethanol	520.2	6.90	534.0	0.90	6.51	1.38	0.15	548	46
methanol	521.3	7.81	534.8	0.77	5.33	1.44	0.43	549	44
ethanol	522.4	7.95	535.2	0.72	5.31	1.35	0.52	552	45
acetone	521.4	7.91	535.2	0.65	4.92	1.32	0.71	549	44
ethyl acetate	521.7	7.91	534.8	0.69	5.08	1.35	0.61	548	43
c-hexane	525.1	8.63	537.2	0.49	3.88	1.26	1.31	552	41

<sup>a</sup> Wavelength of maximum absorption ( $\lambda_{ab}$ ), fluorescence ( $\lambda_{fl}$ ) and laser ( $\lambda_{la}$ ) emission, molar absorption coefficient ( $\epsilon_{max}$ ), and fluorescence quantum yield ( $\phi$ ) and lifetime ( $\tau$ ) as well as percent lasing efficiency (%eff). Concentration:  $2 \times 10^{-6}$  M in absorption and fluorescence data; [PAr1Ac] =  $8.0 \times 10^{-4}$  M and [PAr3Ac] =  $4.5 \times 10^{-4}$  M in lasing data. <sup>b</sup> 2,2,2-Trifluoroethanol.

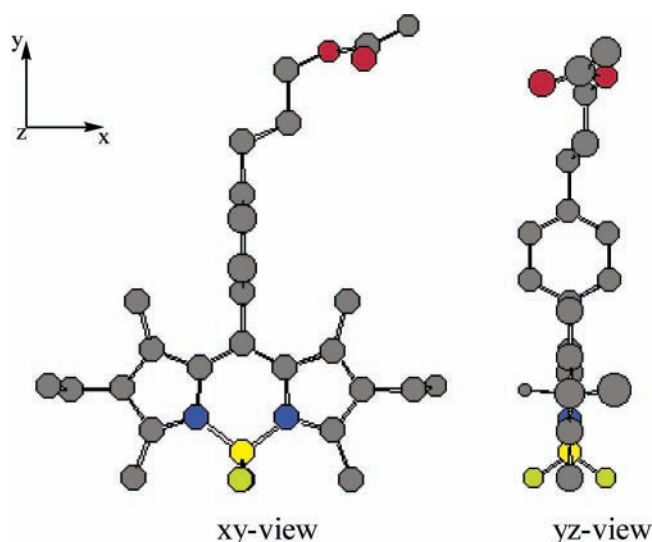


**Figure 3.** Optimized geometry for PAr3Ac obtained by the AM1 semiempirical method in the ground state. The geometry is shown in two perspectives to emphasize the near-perpendicular disposition of the 8-phenyl group with respect to the dipyrromethene·BF<sub>2</sub>  $\pi$  system.

mophoric core and that the acetoxy group is far away from the chromophore, avoiding any possible intra- or intermolecular interaction with the P·BF<sub>2</sub>  $\pi$  system. Similar conclusions were previously reported for the PM567 analogues PnAc, with a linear  $\omega$ -acetoxy polymethylene chain at the 8-position with more than three methylene linking units.<sup>14</sup>

The evolution of the photophysical properties with the solvent for both dyes is nearly the same (Table 1) and is similar to that observed for other P·BF<sub>2</sub> dyes:<sup>14,19</sup> the absorption and fluorescence bands are shifted toward higher energies, and the fluorescence quantum yields and lifetimes increase when changing from apolar to polar protic solvents. These evolutions are related to the influence of the solvent on the stabilization of the resonant structures of P·BF<sub>2</sub> dyes, as discussed elsewhere.<sup>19,33</sup>

The fluorescence quantum yield and lifetime of PAr1Ac and PAr3Ac are lower than those observed for the PM567 dye<sup>22</sup> mainly because of an increase in the probability of the nonradiative processes due to the presence of the phenyl group. The radiative deactivation probability of these 8-aromatic analogues remains high, as reflected in their high molar absorption coefficient. To gain more insight into the nonradiative

deactivation mechanism of the new dyes, the probability of intersystem crossing in PAr1Ac with respect to that in PM567 in aerated benzene solutions was analyzed through the corresponding T–T absorption spectrum as well as the quantum yield of singlet oxygen generation.<sup>34</sup> The results attained from these experiments demonstrated that the spectral characteristics of the T–T absorption band and the formation of singlet oxygen (quantum yields in benzene: 0.090 and 0.078 for PM567 and PAr1Ac, respectively) are similar in both dyes.

The above arguments led to the assignment of the nonradiative deactivation from the excited state to internal conversion processes.<sup>35</sup> The internal conversion of aromatic compounds has been ascribed to the flexibility/rigidity of the molecular structure, which is related, for instance, to a possible rotation of a pendant phenyl group.<sup>28,36</sup> However, as discussed above, the presence of the 8-phenyl group in the PM567 chromophore does not support an extra deactivation channel associated with its rotation. In previous work, it was observed that aromatic solvents (benzene, toluene, etc.) decrease the fluorescence quantum yields of P·BF<sub>2</sub> dyes because of an augmentation of the nonradiative rate constant in these solvents.<sup>19,33</sup> Such an extra internal conversion process could be related to the dissipation of excitation energy through the vibrational movement of the 8-phenyl skeleton.

Because the laser signal is normally obtained in concentrated solutions of dyes, it is interesting to study the photophysical properties of the new compounds under these conditions. Because of the similar photophysical behavior exhibited by both analogues, the dye concentration effect was studied only in PAr1Ac.

Figure 4 shows the absorption and fluorescence spectra of PAr1Ac at different concentrations. The shape of the absorption band is nearly independent of the dye concentration, suggesting that aggregation in this dye is negligible, at least at a concentration of up to  $10^{-3}$  M. This low (if any) aggregation tendency of P·BF<sub>2</sub> dyes is important when pyromethenes dyes are compared with rhodamines as active media in tunable lasers because the aggregation of rhodamines (probably the most commonly used laser dyes) results in efficient quenching of the monomer fluorescence emission.<sup>37</sup> The fluorescence band of PAr1Ac is shifted toward lower energies (Figure 4) in highly concentrated samples when measurements are made in 0.01-cm path length cuvettes. However, the band returns to its position in dilute solutions when the fluorescence spectra are registered using a narrower cuvette (0.001 cm). This dependence

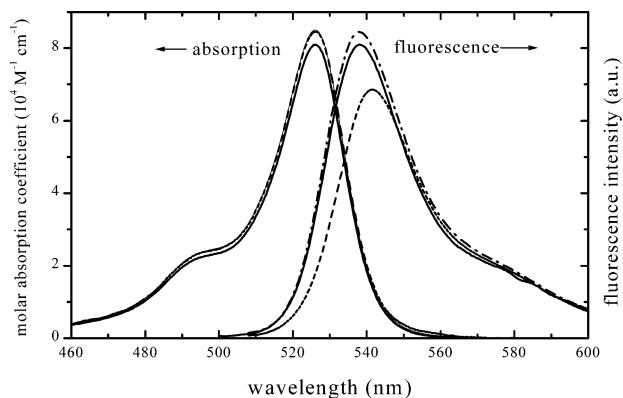


**Figure 4.** Absorption and fluorescence (scaled to the fluorescence quantum yield) spectra of PAR1Ac in cyclohexane: dilute solutions ( $2 \times 10^{-6}$  M) and 1-cm path length cuvettes (—); concentrated solutions ( $10^{-3}$  M) and 0.01-cm (---) and 0.001-cm (- · -) path length cuvettes.

**TABLE 2: Fluorescence Quantum Yields ( $\phi$ ) and Lifetimes ( $\tau$ ) of Concentrated PAR1Ac Solutions ( $10^{-3}$  M) in 0.01- and 0.001-cm Path Length ( $l$ ) Cuvettes<sup>a</sup>**

solvent	$l = 0.01$ cm		$l = 0.001$ cm	
	$\phi$ ( $\phi^b$ ) ( $\pm 0.05$ )	$\tau$ ( $\tau^b$ ) ( $\pm 0.05$ ns)	$\phi$ ( $\pm 0.10$ )	$\tau$ ( $\pm 0.05$ ns)
F <sub>3</sub> -ethanol	0.57 (0.68)	7.67 (6.88)	0.75	6.30
methanol	0.58 (0.68)	6.43 (5.71)	0.75	5.28
ethanol	0.56 (0.66)	6.63 (5.92)	0.64	5.27
acetone	0.55 (0.67)	6.15 (5.33)	0.68	4.90
ethyl acetate	0.55 (0.64)	6.41 (5.67)	0.67	5.16
c-hexane	0.39 (0.48)	4.60 (4.00)	0.46	3.81

<sup>a</sup> Other photophysical properties are not included because they are the same as those obtained in diluted solutions. <sup>b</sup> Values corrected from reabsorption and reemission effects.<sup>3</sup>

of the recorded fluorescence band on the path length of the cuvette suggests an important influence of the reabsorption/reemission effects when high-optical-density solutions are analyzed.<sup>23</sup>

Table 2 lists the fluorescence quantum yields ( $\phi$ ) and lifetimes ( $\tau$ ) in concentrated solutions ( $10^{-3}$  M) with two different optical path length cuvettes in several solvents. The  $\phi$  and  $\tau$  values obtained in the 0.01-cm cuvette are lower and higher, respectively, than the corresponding values recorded in the narrower 0.001-cm cuvette, which are similar to those observed in dilute solutions (Table 1). The influence of reabsorption/reemission phenomena in the  $\phi$  and  $\tau$  values observed in the 0.01-cm cuvette is not completely corrected by mathematical methods,<sup>23</sup> but these phenomena are practically negligible in the 0.001-cm cuvette, although in this case a higher experimental error in the  $\phi$  value is obtained. The augmentation of the dye concentration produces a diminution in the  $\phi$  value in the polar solvent 2,2,2-trifluoroethanol, from 0.81 to 0.75 in concentrated solutions ( $l = 0.001$  cm), and to 0.68 after reabsorption/reemission correction in the 0.01-cm cuvette (fluorescence recorded with high reabsorption/reemission effects). This tendency leads to the equalization of the  $\phi$  value for concentrated solutions in polar media, although the lowest  $\phi$  and  $\tau$  values of PAR1Ac are still obtained in cyclohexane. From this photophysical study, there is no evidence for an intermolecular interaction affecting the photophysical properties of PAR1Ac in the very polar 2,2,2-trifluoroethanol environment.

**Lasing Properties in the Liquid Phase.** The concentrations of PAR1Ac and PAR3Ac in these experiments were  $8 \times 10^{-4}$  and  $4.5 \times 10^{-4}$  M, respectively, leading to solutions with an optical density at the pump laser radiation of ca. 13. It is seen

**TABLE 3: Laser Efficiency (%eff) for the 8-Phenyl Dipyrromethenes Dyes as a Function of the Dye Concentration in Three Representative Solvents**

dye	solvent	[dye] $\times 10^{-3}$ M								
		0.07	0.14	0.20	0.45	0.60	0.80	1.00	1.60	2.00
PAR1Ac	F <sub>3</sub> -EtOH	12	22	38	41	44	40	36		
	EtOH	7	15	31	38	43	41	32		
	c-hexane	1	10	22	37	40	36	29		
PAR3Ac	F <sub>3</sub> -EtOH	11	23	39	46	46	45	43	39	
	EtOH	7	16	33	45	44	44	41	36	36
	c-hexane	8	19	42	41	40	38	33	31	

that these new dyes lase efficiently (Table 1), with energy conversion efficiency nearly solvent-independent, following the same behavior previously observed for other analogues.<sup>13,38</sup>

The dependence of the laser action on the dye concentration was analyzed in 2,2,2-trifluoroethanol, ethanol, and cyclohexane in solutions with optical density in the range of 1.5–35, keeping the other experimental parameters constant (Table 3). As expected, the lasing efficiency of the dyes increases significantly with the concentration, reaching a maximum value for solutions with an optical density of ca. 13. From this point on, further increases in the dye concentration result in a slight decrease in the lasing efficiency. The laser emission is shifted to lower energies as the concentration increases. This trend must be related to the effect of reabsorption/reemission phenomena on the emission intensity and could also be the origin of the decrease in the lasing efficiency observed in the more highly concentrated solutions.<sup>23</sup>

The actual effect of the solvent on the lasing efficiency can be detected only in moderately concentrated samples (optical density  $< 10$ ) and follows the same dependence as that exhibited by PM567: the polar protic nature of the solvent (2,2,2-trifluoroethanol and ethanol) improves the lasing efficiency of the dyes with respect to the values registered in polar nonprotic and apolar solvents. Consequently, and in good agreement with the behavior of the PM567 dye, polar protic solvents such as 2,2,2-trifluoroethanol are recommended as the best liquid media for the laser operation of these new dyes. In addition, for all of the selected solvents and in moderately concentrated solutions, the lasing efficiency increases with the length of the polymethylene chain, following the same behavior as that observed for PnAc dyes.<sup>14</sup>

The lasing characteristics observed in moderately concentrated solutions of PArnAc dyes show good correlations with their photophysical properties in dilute solution. Thus, the highest fluorescence quantum yield was observed in 2,2,2-trifluoroethanol for both homologous, which is related to the highest lasing efficiencies obtained in polar protic solvents. In addition, the lasing efficiency of these new dyes compares well with those obtained for P1Ac, P3Ac, and P5Ac dyes in all of the solvents studied and gives results that are slightly lower than those reached with P10Ac and P15Ac dyes as well as with the difunctionalized analogues.<sup>13,14</sup> This lasing behavior also follows the trend observed in the photophysical properties: the  $\phi$  values of PnAc dyes ( $n = 1, 3,$  and  $5$ ) are similar to those of PArnAc and are slightly lower than those registered for P10Ac and P15Ac dyes.

Despite having both lower  $\phi$  and higher  $k_{nr}$  values, the PArnAc dyes lase more efficiently than the commercial PM567 dye in ethanol, ethyl acetate, acetone, and cyclohexane.<sup>22</sup> The laser emission of the PArnAc dyes shifts up to 13 nm to shorter wavelengths with respect to that of PM567. As a result, laser action in PArnAc complexes takes place at a wavelength closer to its maximum of fluorescence than in the case of PM567, where the laser emission peaked at a wavelength where its

**TABLE 4: Photophysical Parameters of PAr*n*Ac/PMMA and COP(PAr*n*MA-MMA) with *n* = 1 and 3<sup>a</sup>**

material	$\lambda_{ab}$ (nm)	$\epsilon_{max}$ ( $10^4 \text{ M}^{-1} \text{ cm}^{-1}$ )	$\lambda_{fl}$ ( $\lambda_{fl}^b$ ) (nm)	$\phi$ ( $\phi^b$ )	$\tau$ ( $\tau^b$ ) (ns)
PAr1Ac/PMMA	524.7	6.90	546.4 (536.4)	0.69 (0.82)	11.14 (9.37)
COP(PAr1MA-MMA)	524.9	8.00	546.0 (536.8)	0.69 (0.84)	11.35 (9.42)
PAr3Ac/PMMA	523.7	8.36	542.8 (534.4)	0.65 (0.82)	10.62 (8.25)
COP(PAr3MA-MMA)	524.1	8.65	543.2 (535.2)	0.61 (0.80)	10.56 (8.01)

<sup>a</sup> Dye concentration:  $1.5 \times 10^{-3}$  M. Absorption ( $\lambda_{ab}$ ) and fluorescence ( $\lambda_{fl}$ ) wavelengths, molar absorption coefficient ( $\epsilon_{max}$ ), fluorescence quantum yield ( $\phi$ ) and lifetime ( $\tau$ ) for the decay component. <sup>b</sup> Values corrected from reabsorption and reemission effects.<sup>3</sup>

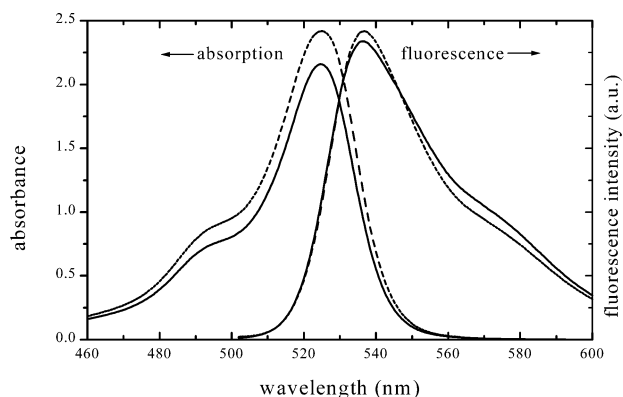


**Figure 5.** Absorption and normalized fluorescence (corrected for reabsorption and reemission effects) spectra of PAr1Ac/PMMA (—) and COP(PAr1MA-MMA) (---).

fluorescence intensity had considerably declined. Consequently, in PAr*n*Ac dyes the laser gain coefficient, which is proportional to the population inversion, is significantly enhanced with respect to that of PM567, performing efficient laser emission despite their photophysical properties.

When the laser signals are obtained in highly concentrated solutions, the laser efficiency becomes independent of the environment, and both the influence of the solvent on the laser emission and the good agreement between photophysics and lasing properties is somewhat lost. The high optical density of these samples, in which the saturation of the excitation beam is more probable and reabsorption/reemission effects must be very important, could lead to this low environmental dependence of the fluorescence and laser intensity.

**Photophysical Properties in the Solid State.** The PAr*n*Ac dyes have been incorporated into a poly(methyl methacrylate) (PMMA) matrix as dopants (PAr1Ac/PMMA and PAr3Ac/PMMA), and their analogues PAr*n*MA have been covalently bound to the PMMA chain (COP(PAr1MA-MMA) and COP(PAr3MA-MMA)). The photophysical properties of all of these solid materials were also measured.

Under the measurement conditions (polymeric disks, dye concentration  $1.5 \times 10^{-3}$  M, and 0.2-mm path length), the reabsorption/reemission phenomena affect the fluorescence properties of these systems. This is corroborated by the obtained decay curves for COP(PAr1MA-MMA) (Figure 2, curve B), where the deconvolution leads to a growing and a decay component. The growing component is explained by a time delay between the excitation pulse and the maximum population of the fluorescence excited state, which is due to consecutive reabsorption/reemission phenomena at the excitation beam. Successive reabsorption/reemission processes at the emission wavelength increase the recorded time in which the molecules are in the excited state (long-lifetime decay component).

Figure 5 shows the absorption and fluorescence (corrected for reabsorption/reemission effects)<sup>23</sup> bands of PAr1Ac/PMMA and COP(PAr1MA-MMA). The spectral bands in polymeric matrices are slightly broader than those obtained in liquid

**TABLE 5: Laser Parameters<sup>a</sup> for 8-Phenyl Dipyrromethene·BF<sub>2</sub> Dyes in PMMA as a Solution (PAr*n*Ac/PMMA, *n* = 1 and 3) or Copolymerized with MMA (COP(PAr*n*MA-MMA))<sup>b</sup>**

material	[c] (mM)	$\lambda_{la}$ (nm)	$\Delta\lambda$ (nm)	%eff	lifetime <sup>c</sup>	
					60 000	100 000
PM567/PMMA	1.5	562	7	12	0	
PAr1Ac/PMMA	0.8	555	8	23	62	
PAr1Ac/PMMA	1.5	558	15	18	73	
COP(PAr1MA/MMA)	0.8	556	5	21		88
COP(PAr1MA/MMA)	1.5	558	9	20		96
PAr3Ac/PMMA	0.45	551	6	21	75	
PAr3Ac/PMMA	1.5	554	12	18	83	
COP(PAr3MA/MMA)	0.45	551	5	20		75
COP(PAr3MA/MMA)	1.5	555	9	16		96

<sup>a</sup>  $\lambda_{la}$ , peak wavelength of the laser emission;  $\Delta\lambda$ , FWHM of the laser emission, %eff, energy-conversion efficiency. <sup>b</sup> Nd:KGW laser (second harmonic) pump energy: 5.5 mJ/pulse; repetition rate: 10 Hz. Data for PM567 are included for comparison. <sup>c</sup> Percent intensity of the dye laser output after *n* pump pulses with reference to the initial intensity.

solution, which is attributed to changes in the vibronic structure of the electronic band in the solid environment. Table 4 lists the photophysical properties of PAr*n*Ac in solid polymers. The peak wavelengths of the absorption and emission bands are close to those obtained in polar solvents, indicating that the framework of the solid polymer does not extensively affect the photophysics of PAr*n*Ac dyes. However, the rigid structure of the polymeric matrices could lead to a reduction in the flexibility of the dye's molecular structure, decreasing the probability of internal conversion and explaining the observed increase in the  $\phi$  values in solid polymers (Table 4) with respect to the values reached in polar liquid solvents (Table 1). Although the covalent linkage of the 8-phenyl P·BF<sub>2</sub> dyes to the polymeric chain does not cause any appreciable modification of the  $\phi$  values, the important improvements formerly observed in the photo- and thermostability of several P·BF<sub>2</sub> dyes bound to polymeric chains<sup>16</sup> led us to study the laser behavior of a number of samples of the new 8-phenyl analogues incorporated into solid matrices of MMA.

**Lasing Properties in the Solid-State.** The experiments were carried out in samples with the same dye concentration as that producing the highest lasing efficiency in liquid solution. To assess the effect of the optical density on laser operation, materials with a higher concentration ( $1.5 \times 10^{-3}$  M) were also prepared, and their lasing properties were registered and compared with those exhibited by other P·BF<sub>2</sub> analogues incorporated into polymeric matrices.<sup>16,37,39</sup>

Broadband and efficient laser emission was obtained from all of the studied materials (Table 5). As the dye concentration increases, the reabsorption/reemission phenomena shift the emission band to lower energies and widen the bandwidths. The 8-phenyl P·BF<sub>2</sub> dyes incorporated into PMMA lase much more efficiently than the PM567 dye under the same conditions. However, the lasing efficiencies of the new dyes, in the range of 16–23%, are somewhat lower than those obtained with other monofunctionalized dipyrromethene dyes dissolved or copoly-

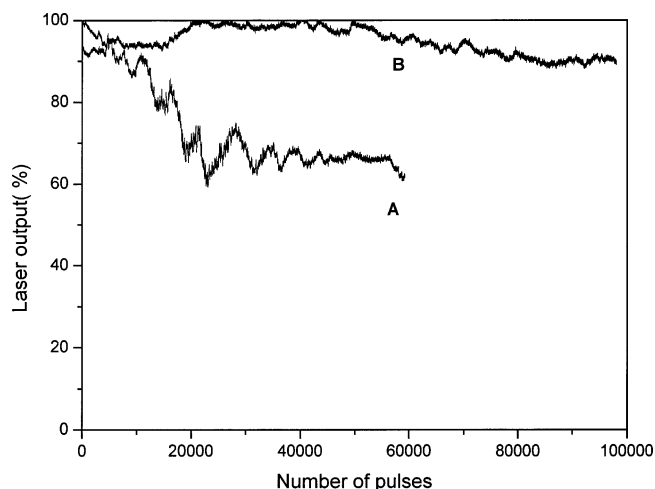


**Figure 6.** Normalized laser output as a function of the number of pump pulses for the PAR1Ac dye dissolved in PMMA, (PAR1Ac/PMMA) (A), and for PAR1MA copolymerized with MMA, COP(PAr1MA/MMA) (B). Dye concentration:  $0.8 \times 10^{-3}$  M. Pump energy and repetition rate: 5.5 mJ/pulse and 10 Hz, respectively.

merized with MMA,<sup>13,37,39</sup> following the same behavior exhibited by the fluorescence quantum yields.

The evolution of the laser output as a function of the number of pump pulses in the same position in the sample was studied for the different materials. The intensities of the laser output after  $n$  pump pulses with reference to the initial intensity of the laser emission ( $I_n$  (%) =  $(I_n/I_0) \times 100$ , where  $I_0$  is the initial intensity), with  $n$  ranging from 60 000 for the model dyes to 100 000 for the copolymer samples, are listed in Table 5.

For the sake of clarity, the evolution of the laser output with the number of pump pulses is shown in Figure 6 for the model dye PAR1Ac/PMMA and the copolymer COP(PAr1MA-MMA). It can be appreciated that the material where the chromophore is covalently bonded to the polymeric chains exhibits a higher photostability than that of the material where the same dye is simply dissolved in the polymer, confirming that the covalent linkage provides additional channels for the elimination of the absorbed pump energy that is not converted into emission, which prevents the accumulation of heat in the material.

For a given concentration, the lasing efficiency and lifetime become nearly independent of the length of the polymethylene linking chain, following the same behavior observed for the fluorescence quantum yield values. In all cases, the increase in the chromophore concentration resulted in a slight decrease in lasing efficiency (correlated with a decrease in the fluorescence quantum yield) but a significant increase in laser photostability because the increased concentration of the dye can compensate to some extent for the photodegradation of the dye molecules caused by the excitation pulses, resulting in apparently enhanced laser photostability.

The lasing stabilities of the new materials studied in this work clearly improve the useful lifetime of PM567 and analogues PnAc and PnMA, all incorporated into PMMA.<sup>16</sup> This enhancement could be related to a higher photochemical stabilization of the chromophore rather than to a decline in the nonradiative deactivation processes because all dyes present similar values for the  $k_{nr}$  rate constant.

#### IV. Conclusions

In this paper, we report efficient and highly photostable laser operation from newly synthesized dipyrromethene·BF<sub>2</sub> dyes, analogues of PM567, in liquid solutions as well as incorporated

into solid polymeric matrices. The presence of an 8-phenyl group in the chromophore leaves the photophysics of the dye practically unmodified so that in liquid solution it depends mainly on the solvent polarity. Very polar protic solvents are recommended as the best liquid media for laser operation because the highest values of the fluorescence quantum yields are obtained in these solvents.

Despite having both lower  $\phi$  and higher  $k_{nr}$  values, the new dyes lase more efficiently than PM567 in solvents such as ethanol, ethyl acetate, acetone, and cyclohexane under the same experimental conditions. The reference dye PM567 exhibited a lasing efficiency of 12% when doped in PMMA, whereas the lasing efficiency of the new materials ranged from 16 to 23%. The emission of PM567 incorporated into PMMA drops to zero after less than 40 000 pump pulses, whereas the laser emission of COP(PAr1MA/MMA) and COP(PAr3MA/MMA) materials remains at 96% of its initial value after 100 000 pump pulses at a 10-Hz repetition rate.

The results presented in this work indicate that appropriate chemical modifications in the dipyrromethene molecules can yield dyes that lase efficiently and with remarkable photostability when properly incorporated into polymeric matrices, rendering materials that can actually compete with the liquid dye lasers and make possible the implementation of a commercial solid-state dye laser.

**Acknowledgment.** This work was supported by Projects MAT2000-1361-C04-01 and MAT2000-1361-C04-02 of the Spanish MCYT. J.B.P. thanks the Universidad del País Vasco for a predoctoral grant. L.C. thanks the CNPq of Brazil for a research grant. Thanks are also given to Professors N. A. García and S. Bertolotti for the determination of quantum yields of singlet oxygen generation.

#### Appendix

**General Methods.** Analytical thin-layer chromatography was performed on silica gel-precoated aluminum foils (Merck 60F254, 0.25 mm). Flash column chromatography was performed on silica gel (Merck, 230–400 mesh). Melting points were measured on a Reichert-Kofler hot-stage microscope and are uncorrected. Yields are reported in reference to isolated pure compounds. <sup>1</sup>H and <sup>13</sup>C NMR spectra were taken on an INOVA-300 spectrometer. Chemical shifts are reported in ppm using as an internal reference the peak of a trace amount of undeuterated solvent or the carbon signal of the deuterated solvent:  $\delta$  7.26 and 77.0 in CDCl<sub>3</sub>. The following abbreviations are used to describe the signals: s (singlet), d (doublet), t (triplet), q (quartet), and m (complex multiplet). Infrared spectra (in cm<sup>-1</sup>) were recorded on a Perkin-Elmer 681 spectrophotometer. Low-resolution mass spectra were recorded by electron impact (70 eV) in a Hewlett-Packard 5973 spectrometer in the direct injection mode. High-resolution mass spectra were determined by electron impact (70 eV) in an AutoSpec Micromass (Waters) apparatus in direct-injection mode (peak matching) with perfluorokerosene as an exact mass standard. UV–vis absorption spectra were registered on a Perkin-Elmer Lambda-16 spectrophotometer.

**PAR1Cl:** Red crystals; yield 27%; mp 172–174 °C. <sup>1</sup>H NMR (300 MHz, CDCl<sub>3</sub>, 25 °C):  $\delta$  0.89 (t,  $J$  = 7.5 Hz, 6 H, 2 × CH<sub>3</sub>CH<sub>2</sub>), 1.2 (s, 6 H, CH<sub>3</sub>–C1, CH<sub>3</sub>–C7), 2.21 (q,  $J$  = 7.5 Hz, 4 H, 2 × CH<sub>3</sub>CH<sub>2</sub>), 2.44 (s, 6 H, CH<sub>3</sub>–C3, CH<sub>3</sub>–C5), 4.58 (s, 2 H, CH<sub>2</sub>Cl), 7.19 (d,  $J$  = 8.2 Hz, 2 H, 2 × *H*-Ar), 7.42 (d,  $J$  = 8.2 Hz, 2 H, 2 × *H*-Ar). <sup>13</sup>C NMR (75 MHz, CDCl<sub>3</sub>, 25 °C):  $\delta$  11.6 (CH<sub>3</sub>Ar), 12.4 (CH<sub>3</sub>–Ar), 14.4 (CH<sub>3</sub>CH<sub>2</sub>), 17.0

(CH<sub>3</sub>CH<sub>2</sub>), 45.5 (CH<sub>2</sub>Cl), 128.7 (CH-3', CH-5'), 129.0 (CH-2', CH-6'), 130.6 (C-7a, C-8a), 132.8 (C-2, C-6), 135.8 (C-4'), 136.1 (C-1'), 138.4 (C-1, C-7), 139.4 (C-8), 153.8 (C-3, C-5). MS EI *m/z* (%): 428 (nominal mass, M<sup>+</sup>) (96), 413 (100), 393 (9), 363 (6), 196 (8), 189 (8). IR (KBr)  $\nu_{\max}$ : 1540, 1474, 1319, 1192, 1177, 997 cm<sup>-1</sup>. UV-vis (EtOH)  $\lambda_{\max}$  ( $\epsilon$ , M<sup>-1</sup>cm<sup>-1</sup>): 376 (7850), 523 (81 800) nm.

**Par3Br:** Red crystals; yield 32%; mp 156–158 °C. <sup>1</sup>H NMR (300 MHz, CDCl<sub>3</sub>, 25 °C):  $\delta$  0.89 (t, *J* = 7.5 Hz, 6 H, 2 × CH<sub>3</sub>CH<sub>2</sub>), 1.25 (s, 6 H, CH<sub>3</sub>-C1, CH<sub>3</sub>-C7), 2.22–2.12 (m, 2 H, CH<sub>2</sub>CH<sub>2</sub>Br), 2.27 (q, *J* = 7.5 Hz, 4 H, 2 × CH<sub>3</sub>CH<sub>2</sub>), 2.50 (s, 6 H, CH<sub>3</sub>-C3, CH<sub>3</sub>-C5), 2.85 (t, *J* = 7.2 Hz, 2 H, CH<sub>2</sub>-C4''), 3.37 (t, *J* = 6.5 Hz, 2 H, CH<sub>2</sub>Br), 7.17 (d, *J* = 8.2 Hz, 2 H, 2 × *H*-Ar), 7.29 (d, *J* = 8.2 Hz, 2 H, 2 × *H*-Ar). <sup>13</sup>C NMR (75 MHz, CDCl<sub>3</sub>, 25 °C):  $\delta$  11.6 (CH<sub>3</sub>Ar), 12.4 (CH<sub>3</sub>Ar), 14.6 (CH<sub>3</sub>CH<sub>2</sub>), 17.0 (CH<sub>3</sub>CH<sub>2</sub>), 32.77 ((CH<sub>2</sub>Br), 33.80 (CH<sub>2</sub>-C4''), 34.1 (CH<sub>2</sub>CH<sub>2</sub>Br), 128.5 (CH-3', CH-5'), 129.3 (CH-2', CH-6'), 130.9 (C-7a, C-8a), 132.8 (C-2, C-6), 133.7 (C-1'), 138.4 (C-1, C-7), 140.1 (C-8), 141.3 (C-4'), 153.0 (C-3, C-5). MS EI *m/z* (%): 500 (nominal mass, M<sup>+</sup>) (100), 485 (85), 405 (16), 378 (13), 196 (13). IR (KBr)  $\nu_{\max}$ : 1538, 1474, 1187, 976 cm<sup>-1</sup>.

**Par1Ac:** Red crystals; yield 65%; mp 174–176 °C. <sup>1</sup>H NMR (300 MHz, CDCl<sub>3</sub>, 25 °C):  $\delta$  0.97 (t, *J* = 7.5 Hz, 6 H, 2 × CH<sub>3</sub>CH<sub>2</sub>), 1.29 (s, 6 H, CH<sub>3</sub>-C1, CH<sub>3</sub>-C7), 2.17 (s, 3 H, CH<sub>3</sub>CO), 2.31 (q, *J* = 7.7 Hz, 4 H, 2 × CH<sub>3</sub>CH<sub>2</sub>), 2.54 (s, 6 H, CH<sub>3</sub>-C3, CH<sub>3</sub>-C5), 5.22 (s, 2 H, CH<sub>2</sub>O), 7.29 (d, *J* = 8.1 Hz, 2 H, 2 × *H*-Ar), 7.49 (d, *J* = 8.0 Hz, 2 H, 2 × *H*-Ar). <sup>13</sup>C NMR (75 MHz, CDCl<sub>3</sub>, 25 °C):  $\delta$  11.7 (CH<sub>3</sub>Ar), 12.4 (CH<sub>3</sub>-Ar), 14.5 (CH<sub>2</sub>CH<sub>3</sub>), 17.0 (CH<sub>2</sub>CH<sub>3</sub>), 21.0 (CH<sub>3</sub>CO), 65.6 (CH<sub>2</sub>O), 128.4 (CH-3', CH-5'), 128.5 (CH-2', CH-6'), 130.7 (C-7a, C-8a), 132.8 (C-2, C-6), 135.6 (C-4'), 136.8 (C-1'), 138.8 (C-1, C-7), 139.6 (C-8), 153.8 (C-3, C-5), 170.8 (C=O). MS EI *m/z* (%): 452 (nominal mass, M<sup>+</sup>) (95), 437 (100), 423 (9), 393 (15), 189 (4). HRMS (EI): calcd for C<sub>26</sub>H<sub>31</sub>BF<sub>2</sub>N<sub>2</sub>O<sub>2</sub>, 452.2447; found, 452.2454. IR (KBr)  $\nu_{\max}$ : 1740, 1541, 1476, 1192, 979 cm<sup>-1</sup>.

**Par3Ac:** Orange crystals; yield 73%; mp 128–130 °C. <sup>1</sup>H NMR (300 MHz, CDCl<sub>3</sub>, 25 °C):  $\delta$  0.97 (t, *J* = 7.5 Hz, 6 H, 2 × CH<sub>3</sub>CH<sub>2</sub>), 1.28 (s, 6 H, CH<sub>3</sub>-C1, CH<sub>3</sub>-C7), 1.98–2.05 (m, 2 H, CH<sub>2</sub>CH<sub>2</sub>O), 2.09 (s, 3 H, CH<sub>3</sub>CO), 2.29 (q, *J* = 7.5 Hz, 4 H, 2 × CH<sub>3</sub>CH<sub>2</sub>), 2.52 (s, 6 H, CH<sub>3</sub>-C3, CH<sub>3</sub>-C5), 2.78 (t, *J* = 7.6 Hz, 2 H, CH<sub>2</sub>-C4''), 4.08 (t, *J* = 6.6 Hz, 2 H, CH<sub>2</sub>O), 7.19 (d, *J* = 8.1 Hz, 2 H, 2 × *H*-Ar), 7.29 (d, *J* = 8.1 Hz, 2 H, 2 × *H*-Ar). <sup>13</sup>C NMR (75 MHz, CDCl<sub>3</sub>, 25 °C):  $\delta$  11.6 (CH<sub>3</sub>-Ar), 12.5 (CH<sub>3</sub>Ar), 14.6 (CH<sub>3</sub>CH<sub>2</sub>), 17.0 (CH<sub>3</sub>CH<sub>2</sub>), 21.0 (CH<sub>3</sub>-CO), 33.2, 31.9 (PhCH<sub>2</sub>CH<sub>2</sub>), 63.5 (CH<sub>2</sub>O), 128.3 (CH-3', CH-5'), 128.9 (CH-2', CH-6'), 130.8 (C-7a, C-8a), 132.7 (C-2, C-6), 133.5 (C-1'), 138.4 (C-1, C-7), 140.0 (C-8), 141.8 (C-4'), 153.5 (C-3, C-5), 176 (C=O). MS EI *m/z* (%): 480 (nominal mass, M<sup>+</sup>) (100), 465 (71), 405 (6), 391 (6). HRMS (EI): calcd for C<sub>28</sub>H<sub>35</sub>BF<sub>2</sub>N<sub>2</sub>O<sub>2</sub>, 480.2760; found, 480.2761. IR (KBr)  $\nu_{\max}$ : 1737, 1539, 1476, 1188, 978 cm<sup>-1</sup>.

**Par1MA:** Orange crystals; yield 52%; mp 115–117 °C. <sup>1</sup>H NMR (300 MHz, CDCl<sub>3</sub>, 25 °C):  $\delta$  0.98 (t, *J* = 7.7 Hz, 6 H, 2 × CH<sub>3</sub>CH<sub>2</sub>), 1.28 (s, 6 H, CH<sub>3</sub>-C1, CH<sub>3</sub>-C7), 2.00 (m, 3 H, CH<sub>3</sub>C=CH<sub>2</sub>), 2.30 (q, *J* = 7.7 Hz, 4 H, 2 × CH<sub>3</sub>CH<sub>2</sub>), 2.53 (s, 6 H, CH<sub>3</sub>-C3, CH<sub>3</sub>-C5), 5.30 (s, 2 H, CH<sub>2</sub>O), 5.64 (m, 2 H, CHH=C), 6.2 (m, 2 H, CHH=C), 7.26 (d, *J* = 7.8 Hz, 2 H, 2 × *H*-Ar), 7.49 (d, *J* = 7.8 Hz, 2 H, 2 × *H*-Ar). <sup>13</sup>C NMR (75 MHz, CDCl<sub>3</sub>, 25 °C):  $\delta$  11.6 (CH<sub>3</sub>Ar), 12.4 (CH<sub>3</sub>Ar), 14.1 (CH<sub>3</sub>CH<sub>2</sub>), 17.0 (CH<sub>3</sub>CH<sub>2</sub>), 18.3 (CH<sub>3</sub>C=CH<sub>2</sub>), 65.7 (CH<sub>2</sub>O), 125.9 (CH<sub>2</sub>=C), 128.1 (CH-3', CH-5'), 128.5 (CH-2', CH-6'), 130.8 (C-7a, C-8a), 132.8 (C-2, C-6), 135.5 (C-4'), 136.1 (C-1'), 136.9 (CH<sub>3</sub>C=CH<sub>2</sub>), 138.3 (C-1, C-7), 139.6 (C-8), 153.7

(C-3, C-5), 167.0 (C=O). MS EI *m/z* (%): 479 (nominal mass, M<sup>+</sup>) (31), 478 (100), 463 (82), 393 (10), 378 (6), 189 (4). HRMS (EI): calcd for C<sub>28</sub>H<sub>33</sub>BF<sub>2</sub>N<sub>2</sub>O<sub>2</sub>, 478.2603; found, 478.2604. IR (KBr)  $\nu_{\max}$ : 1721, 1540, 1474, 1315, 1185, 977 cm<sup>-1</sup>.

**Par3MA:** Orange crystals; yield 55%; mp 120–121 °C. <sup>1</sup>H NMR (300 MHz, CDCl<sub>3</sub>, 25 °C):  $\delta$  0.98 (t, *J* = 7.5 Hz, 6 H, 2 × CH<sub>3</sub>CH<sub>2</sub>), 1.29 (s, 6 H, CH<sub>3</sub>-C1, CH<sub>3</sub>-C7), 2.04 (m, 3 H, CH<sub>3</sub>C=CH<sub>2</sub>), 1.99–2.04 (m, 2 H, CH<sub>2</sub>CH<sub>2</sub>O), 2.30 (q, *J* = 7.5 Hz, 4 H, 2 × CH<sub>3</sub>CH<sub>2</sub>), 2.53 (s, 6 H, CH<sub>3</sub>-C3, CH<sub>3</sub>-C5), 4.17 (t, *J* = 7.6 Hz, 2 H, CH<sub>2</sub>-C4''), 4.17 (t, *J* = 6.6 Hz, 2 H, CH<sub>2</sub>O), 5.60 (m, 2 H, CHH=CH<sub>2</sub>), 6.16 (m, 2 H, CHH=CH<sub>2</sub>), 7.19 (d, *J* = 8.0 Hz, 2 H, 2 × *H*-Ar), 7.31 (d, *J* = 8.0 Hz, 2 H, 2 × *H*-Ar). <sup>13</sup>C NMR (75 MHz, CDCl<sub>3</sub>, 25 °C):  $\delta$  11.6 (CH<sub>3</sub>Ar), 12.3 (CH<sub>3</sub>Ar), 14.5 (CH<sub>3</sub>CH<sub>2</sub>), 17.0 (CH<sub>3</sub>CH<sub>2</sub>), 18.5 (CH<sub>3</sub>C=CH<sub>2</sub>), 31.8, 30.1 (CH<sub>2</sub>CH<sub>2</sub>-C4''), 60.2 (CH<sub>2</sub>O), 125.3 (CH<sub>2</sub>=C), 128.2 (CH-3', CH-5'), 128.9 (CH-2', CH-6'), 130.8 (C-7a, C-8a), 132.6 (C-2, C-6), 133.4 (C-1'), 136.3 (CH<sub>3</sub>C=CH<sub>2</sub>), 138.3 (C-1, C-7), 140.2 (C-8), 141.8 (C-4'), 153.4 (C-3, C-5), 167.2 (C=O). MS EI *m/z* (%): 506 (nominal mass, M<sup>+</sup>) (100), 491 (55), 405 (10), 391 (11), 378 (5). HRMS (EI): calcd for C<sub>30</sub>H<sub>37</sub>BF<sub>2</sub>N<sub>2</sub>O<sub>2</sub>, 506.2916; found, 506.2912. IR (KBr)  $\nu_{\max}$ : 1718, 1542, 1477, 1321, 1194, 980 cm<sup>-1</sup>.

## References and Notes

- Pavlopoulos, T. G.; Shah, M.; Boyer, J. H. *Opt. Commun.* **1989**, *70*, 425.
- Shah, M.; Thangaraj, K.; Soong, M. L.; Wolford, L. T.; Boyer, J. H.; Politzer, I. R.; Pavlopoulos, T. G. *Heteroat. Chem.* **1990**, *1*, 389.
- Pavlopoulos, T. G.; Boyer, J. H.; Shah, M.; Thangaraj, K.; Soong, M. L. *Appl. Opt.* **1990**, *29*, 3885.
- Boyer, J. H.; Haag, A. M.; Soong, M. L.; Thangaraj, K.; Pavlopoulos, T. G. *Appl. Opt.* **1991**, *30*, 3788.
- Boyer, J. H.; Haag, A. M.; Sathyamoorthi, G.; Soong, M. L.; Thangaraj, K.; Pavlopoulos, T. G. *Heteroat. Chem.* **1993**, *4*, 39.
- Partridge, W. P.; Laurendeau, M. N.; Johnson, C. C.; Steppell, R. N. *Opt. Lett.* **1994**, *19*, 1630.
- Pavlopoulos, T. G.; Boyer, J. H.; Thangaraj, K.; Sathyamoorthi, G.; Shah, M. P.; Soong, M. L. *Appl. Opt.* **1992**, *31*, 7089.
- O'Neil, M. P. *Opt. Lett.* **1993**, *18*, 37.
- Rahn, M. D.; King, T. A.; Gorman, A.; Hamblett, I. *Appl. Opt.* **1997**, *36*, 5862.
- Zeng, H.; Liang, F.; Sun, Z.; Yuan, Y.; Yao, Z.; Su, Z. *J. Opt. Soc. Am. B* **2002**, *19*, 1349.
- Costela, A.; García-Moreno, I.; Sastre, R. In *Handbook of Advanced Electronic and Photonic Materials and Devices*; Nalwa, H. S., Ed.; Academic Press: San Diego, CA, 2001; Vol. 7, p 161.
- Pavlopoulos, T. G. *Prog. Quantum Electron.* **2002**, *26*, 193.
- Costela, A.; García-Moreno, I.; Gómez, C.; Amat-Guerri, F.; Sastre, R. *Appl. Phys. Lett.* **2001**, *79*, 305.
- Costela, A.; García-Moreno, I.; Gómez, C.; Sastre, R.; Amat-Guerri, F.; Liras, M.; López Arbeloa, F.; Bañuelos Prieto, J.; López Arbeloa, I. *J. Phys. Chem. A* **2002**, *106*, 7736.
- Amat-Guerri, F.; Liras, M.; Carrascoso, M. L.; Sastre, R. *Photochem. Photobiol.* **2003**, *77*, 577.
- López Arbeloa, F.; Bañuelos Prieto, J.; López Arbeloa, I.; Costela, A.; García-Moreno, I.; Gómez, C.; Amat-Guerri, F.; Liras, M.; Sastre, R. *Photochem. Photobiol.* **2003**, *78*, 30.
- Liang, F.; Zeng, H.; Sun, Z.; Yuan, Y.; Yao, Z.; Xu, Z. *J. Opt. Soc. Am. B* **2001**, *18*, 1841.
- Bodwell, G. J.; Li, J.; Miller, D. O. *Tetrahedron* **1999**, *55*, 12939.
- Foreman, E. L.; McElvain, S. M. *J. Am. Chem. Soc.* **1940**, *62*, 1435.
- Smith, J. H.; Menger, F. M. *J. Org. Chem.* **1969**, *34*, 77.
- Costela, A.; García-Moreno, I.; Gómez, C.; García, O.; Sastre, R. *J. Appl. Phys.* **2001**, *90*, 3159.
- López Arbeloa, F.; López Arbeloa, T.; López Arbeloa, I.; García-Moreno, I.; Costela, A.; Sastre, R.; Amat-Guerri, F. *Chem. Phys.* **1998**, *236*, 331.
- López Arbeloa, I. *J. Photochem.* **1980**, *14*, 97.
- Costela, A.; García-Moreno, I.; Sastre, R.; López Arbeloa, F.; López Arbeloa, T.; López Arbeloa, I. *Appl. Phys. B* **2001**, *73*, 19.
- Wada, M.; Ito, S.; Uno, H.; Murashima, T.; Ono, N.; Urano, Y. *Tetrahedron Lett.* **2001**, *42*, 6711.
- Rurack, K.; Kollmannsberger, M.; Resch-Genger, U.; Daub, J. *J. Am. Chem. Soc.* **2000**, *122*, 968.



- (27) Alonso, M.; Amat-Guerri, F.; Chana, A.; Liras, M.; Maestro, M. A.; Herradon, B. Submitted for publication.
- (28) Kollmannsberger, M.; Gareis, T.; Heinl, S.; Breu, J.; Daub, J. *Angew. Chem., Int. Ed. Engl.* **1997**, *36*, 1333.
- (29) Kollmannsberger, M.; Rurack, K.; Resch-Genger, U.; Daub, J. *J. Phys. Chem. A* **1998**, *102*, 10211.
- (30) Li, F.; Yang, S. I.; Ciringh, Y.; Seth, J.; Martin, C. H.; Singh, D. L.; Kim, D.; Birge, R. R.; Bocian, D. F.; Holten, D.; Lindsey, J. S. *J. Am. Chem. Soc.* **1998**, *120*, 10001.
- (31) Chen, J.; Burghart, A.; Derecskei-Kovacs, A.; Burgess, K. *J. Org. Chem.* **2000**, *65*, 2900.
- (32) López Arbeloa, F.; López Arbeloa, T.; López Arbeloa, I. *J. Photochem. Photobiol., A* **1999**, *121*, 177.
- (33) López Arbeloa, T.; López Arbeloa, F.; López Arbeloa, I.; García-Moreno, I.; Costela, A.; Sastre, R.; Amat-Guerri, F. *Chem. Phys. Lett.* **1999**, *299*, 315.
- (34) García, N. A.; Bertolli, S. Private communication.
- (35) Toele, P.; Zhang, H.; Trieflinger, C.; Daub, J.; Glasbeek, M. *Chem. Phys. Lett.* **2003**, *368*, 66.
- (36) Drexhage, K. H. In *Dye Laser Topics*; Schäffer, F. P., Ed.; Springer: Berlin, 1990; Vol. 1, p 187.
- (37) López Arbeloa, F.; Ruiz Ojeda, P.; López Arbeloa, I. *J. Photochem. Photobiol. A* **1988**, *45*, 313.
- (38) García-Moreno, I.; Costela, A.; Amat-Guerri, F.; Gutierrez, C.; Liras, M.; Sastre, R.; Campo, L. Submitted for publication.
- (39) Costela, A.; García-Moreno, I.; Gómez, C.; Amat-Guerri, F.; Liras, M.; Sastre, R. *Appl. Phys. B* **2003**, *76*, 365.